

## SPODUMENE – PETALITE – EUCRYPTITE: MUTUAL RELATIONSHIPS AND PATTERN OF ALTERATION IN LI-RICH APLITE–PEGMATITE DYKES FROM NORTHERN PORTUGAL

BERNARD CHAROY<sup>§</sup>

*Ecole Normale Supérieure de Géologie, CRPG–CNRS, BP 20, F-54501 Vandoeuvre-lès-Nancy Cedex, France*

FERNANDO NORONHA<sup>§</sup> AND ALEXANDRE LIMA<sup>§</sup>

*Centro de Geologia, Faculdade de Ciências da Universidade do Porto, 4050 Porto, Portugal*

### ABSTRACT

The co-occurrence, at the thin section scale, of the three anhydrous Li-aluminosilicates spodumene, petalite and eucryptite, is not a common feature. Such an association occurs in some aplite–pegmatite dykes of the Covas de Barroso district, northern Portugal. We describe their mutual relationships: where spodumene is an early magmatic phase, petalite precipitates directly from a late orthomagmatic fluid, the spodumene remaining metastably, whereas eucryptite is obviously hydrothermal and secondary. Replacement of the primary Li-minerals is the rule, but is diversified and selective: spodumene is mainly replaced by albite and muscovite, petalite by K-feldspar and eucryptite. Muscovite is widespread, and the late hydrothermal paragenesis is dominated by quartz associated with various mixtures of phosphates. The assemblage eucryptite, K-feldspar and albite is obviously in chemical disequilibrium with the early phases. The compositional evolution of the hydrothermal fluids (Na, K, Li) is tentatively bracketed. There is disequilibrium among thermodynamically conflicting mineral phases in terms of pressure, temperature and fluid:rock ratio, in a mobile and partly open system. A genetic affiliation of the Li-enriched pegmatites with the nearby two-mica granites is difficult to prove. The tectonically controlled intrusion of biotite granites to the east of the pegmatite belt would seem to be responsible of the drop in pressure that accounts for the spodumene–petalite transition and the development of the widespread replacement by feldspars, not present in the western part of the belt.

*Keywords:* granitic pegmatite, spodumene, petalite, eucryptite, replacement by feldspars, Covas de Barroso, Portugal.

### SOMMAIRE

La cohabitation, à l'échelle de la lame mince, des trois phases lithinifères spodumène, pétalite et eucryptite n'est pas une observation très fréquente. Un tel assemblage s'observe dans quelques associations aplite–pegmatite de la région de Covas de Barroso, dans le nord du Portugal. Nous décrivons leurs relations mutuelles. Si le spodumène est manifestement une phase magmatique précoce, la pétalite précipite à partir d'un fluide orthomagmatique, expulsé lors d'une chute de pression, le spodumène demeurant métastable. L'eucryptite est franchement hydrothermale et secondaire. Le remplacement des phases lithinifères précoces est la règle, et il est sélectif: le spodumène essentiellement par l'albite et la muscovite, la pétalite par le feldspath potassique et l'eucryptite. La muscovite secondaire est omniprésente, et le quartz domine la paragenèse hydrothermale tardive, en association avec différents phosphates. L'eucryptite et les deux feldspaths sont de toute évidence en déséquilibre chimique avec les phases lithinifères plus précoces. L'évolution de la composition (en termes de Na, K et Li) des fluides hydrothermaux est approchée. Nos observations démontrent le large déséquilibre entre des phases thermodynamiquement contrastées en termes de pression, température et rapport fluide : roche, dans un système mobile et partiellement ouvert. Si la filiation génétique des pegmatites minéralisées avec les granites à deux micas voisins ne peut être affirmée, l'intrusion tectoniquement contrôlée de granites à biotite à l'est du champ pegmatitique serait responsable de la chute de pression justifiant la transition spodumène–pétalite et le déclenchement d'un remplacement par les feldspaths, absents dans la partie ouest du champ filonien.

*Mots-clés:* pegmatite granitique, spodumène, pétalite, eucryptite, remplacement par les feldspaths, Covas de Barroso, Portugal.

---

<sup>§</sup> *E-mail addresses:* bcharoy@crpg.cnrs-nancy.fr, fmnoronh@fc.up.pt, allima@fc.up.pt

## INTRODUCTION

Granitic pegmatites of the rare-element class constitute only a very minor percentage (less than 2%) of the numerous dykes present in a regional pegmatite population (Stewart 1978, Černý 1993). Li-rich granitic pegmatites are affiliated with the LCT (*i.e.*, Li–Cs–Ta) family (Černý 1982, 1991a) within this class. Silicates (spodumene, petalite, lepidolite and, less commonly, eucryptite) and phosphates (mainly of the amblygonite–montebrasite and lithiophylite–triphylite series) are the main carriers of Li. Depending on pressure, both spodumene and petalite have been experimentally shown to be stable liquidus phases (Fenn 1986). Spatial and temporal relationships between these phases have been tentatively established by Heinrich (1948), Cameron *et al.* (1949), Ginsburg & Gushchina (1954), Stewart (1978), Norton (1983) and Ginsburg (1984). Following the experimental work of Stewart (1978), London (1984) has successfully demonstrated the use of a Li-aluminosilicate grid to constrain the P–T path of crystallization for such Li-rich pegmatites. However, mineral replacements affecting primary Li-rich phases are widespread in the presence of fluids released late in the crystallization (Černý 1972, London & Burt 1982a). Alteration of petalite and spodumene to a mixture of eucryptite, albite, K-feldspar and white mica is the normal consequence of re-equilibration in a restricted system (London & Burt 1982a, Wood & Williams-Jones 1993). “Pegmatite stews in its own juice” (Jahns 1982).

Three examples of Portuguese Li-rich aplite–pegmatite dykes from a larger population of pegmatite bodies were selected for this study, in order to constrain the conditions of the magmatic stage and the steps of hydrothermal re-equilibration. We seek to establish how, when and under what conditions were these Li-aluminosilicates formed and altered. The purpose of this study is: 1) to establish the process of aplite–pegmatite formation, 2) to make comprehensive statements about the steps in the development and evolution of these pegmatites, 3) to summarize the mineralogical features of the different Li-aluminosilicate phases and to establish their chronological relations, 4) to determine the nature of their replacement assemblages, and 5) to evaluate changes in the chemistry of the hydrothermal fluids with time and with falling temperature and pressure.

## GEOLOGICAL SETTING

The Covas de Barroso district (CDB for short), Alto Tâmega, northern Portugal, contains a large population of several dozens of aplite–pegmatite dykes (Fig. 1). These bodies are hosted by low- to medium-grade metasedimentary rocks of Silurian age of the Middle Galicia Tras-os-Montes geotectonic zone (Ribeiro *et al.* 1979). Three phases of Hercynian deformation ( $D_1$  to

$D_3$ ), leading to three superimposed schistosities ( $S_1$  to  $S_3$ ), have been recognized (Noronha *et al.* 1981). Several types of granite bodies are present in the vicinity of the pegmatite belt (Fig. 1). They differ in mineralogy (biotite or two-mica) and timing (deformed or undeformed) with regard to these episodes of deformation. On the basis of their macroscopic fabric due to deformation by post-consolidation stress, the aplite–pegmatite dykes are considered older than the youngest unfoliated, post-tectonic, post- $D_3$  biotite granites (Ferreira *et al.* 1987). The common pegmatites scattered throughout the two-mica granites (interior pegmatites) will not be considered in this study.

Two types of aplite–pegmatite dykes, both cross-cutting the metasediments, are encountered in the CDB district. The first type is represented by countless, thin (meter-size, on average), mainly aplitic dykes and veins, which contain low-grade (<3 kg/t) cassiterite mineralization and are commonly converted to kaolinite. They will not be considered further. The second type is composed of larger aplite–pegmatite dykes. This group of pegmatites is unevenly distributed. Local swarms of several dykes of various size can be traced continuously for a few hundred meters (up to 1 km) along strike, and up to 100 meters (where flat) in outcrop width. Their average thickness (quantifiable only in a few cases) is variable, from less than a few meters up to ten meters across. All pegmatite dykes display irregular patterns in outcrop: some are flat-lying, others have gently or steeply dipping attitudes along strike. The largest usually pinch and swell in accordance with the ductility of their host rocks. A large majority of these dykes exhibits a fracture control, which would seem to indicate the ascent of the pegmatite-forming magma along dilation zones or preferential structural planes in enclosing schists during and after the peak of metamorphism (Brisbin 1986, Černý 1991b). Irregularities (branching or bulging) that occur in the shape of the dykes may result from irregularities in the pattern of the fractures. The orientations of the dykes are mainly controlled by the  $S_2$  foliation, which has been locally deformed by  $S_3$  (crenulation with subvertical axial planes striking at  $120^\circ\text{E}$  on average).

The internal structure of the dykes is not easy to establish at the outcrop scale, owing to chemical weathering. All of them are texturally composite with aplitic and largely granular pegmatitic components. Both textures are intermixed together in variable proportions and spatial relations, and appear to be contemporaneous. Overall, the dykes seem internally unzoned in texture. Aplitic zones are uniform, with only a few tapered K-feldspar phenocrysts present. An aborted comb-layered fabric involving elongate crystals of alkali feldspars may be sporadically encountered. Contacts between pegmatite bodies and enclosing schists are sharp. The host micaceous schists at the footwall are commonly very disturbed, strongly folded and silicified, suggesting a

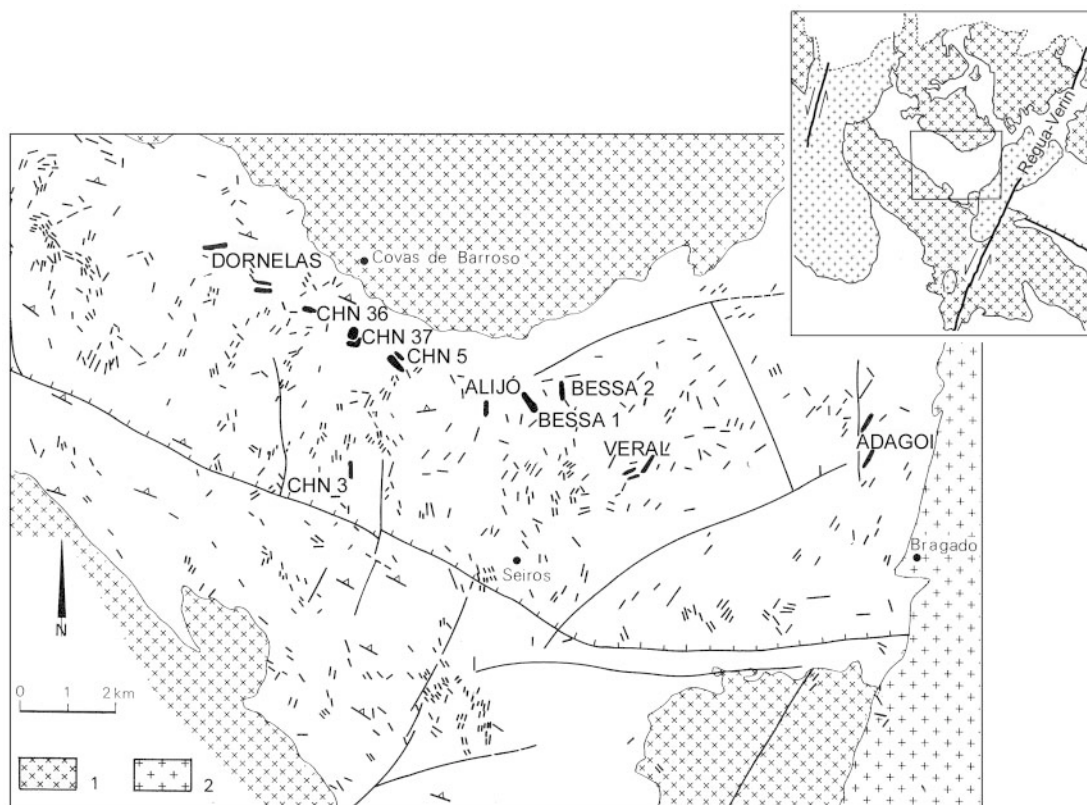


FIG. 1. Geological sketch-map of the Covas de Barroso (CDB) district in northern Portugal, showing the pegmatite belt and the various marginal intrusions of granite. The Li-rich aplite–pegmatite dykes are shown in bold. 1) Syntectonic two-mica granites; 2) post-tectonic (post- $D_3$ ) biotite granites. Insert: regional geology for location of the Rêgua–Verin fault system.

forcible emplacement of the dykes (Brisbin 1986). Flat enclaves (up to half a meter in diameter) of micaceous schists structurally similar to those of the footwall are occasionally enclosed in the pegmatite bodies, commonly with a reaction rim of recrystallized biotite. There is no visible metasomatic alteration of the walls.

Only a few of these large aplite–pegmatite dykes contain spodumene (Charoy *et al.* 1992), but a broader detailed field-based investigation is in progress to establish the distribution of spodumene. Among the bodies of Li-enriched granitic pegmatites already recognized in the CDB district, three of them (Alijó: ALJ, Veral and Adagoi: ADG; Fig. 1) seem to encompass much of the variations in mineralogy of the Li-rich species, mineral sequence and alteration patterns; they were chosen for a trench and drilling program by IGM (Instituto Geológico e Mineiro, Portugal). Our detailed petrographic analysis was conducted on numerous samples from outcrops and drill cores taken from these three occurrences.

## THE LI-BEARING ALUMINOSILICATES

### *Field aspects*

The assemblage of rock-forming minerals in these Li-rich aplite–pegmatites seems fairly simple and granitic in bulk composition. At the outcrop scale, the pegmatitic assemblage consists of: 1) blocky euhedral phenocrysts of feldspar, mostly K-feldspar (as much as 20 cm long), randomly distributed, but locally in scattered clusters or pods; the K-feldspar does not form a graphic texture, as is commonly encountered in margins of numerous granitic pegmatites. 2) Spodumene forms isolated laths or rectangular, radiate or shapeless aggregates. 3) Quartz is found in minor rounded blebs or in intergranular distribution. 4) Muscovite, in centimetric flakes, is subordinate. All are mixed with a minor saccharoidal aplitic matrix with albite, quartz and muscovite. Spodumene is homogeneously distributed within

the pegmatitic differentiates throughout the dykes, but seems significantly enriched near the hanging wall (Fig. 2). The bulk of the spodumene occurs as long blades of euhedral to subhedral crystals, pearly in color, up to 15 cm long (mainly about 5 cm), in parallel growth (columnar aggregates intermixed with quartz) or at random. Aggregates of smaller ragged crystals of spodumene are interstitial between the feldspar megacrysts. Drill cores have intersected a few definite layers (several centimeters across) in which spodumene laths (up to 5 cm long), with a rough branching habit, would suggest a solid-liquid interface.

#### *Petrographic description*

K-feldspar phenocrysts are turbid and have no (or very few) exsolution lamellae of albite, but they do contain albite laths from the matrix as inclusions. The cloudy appearance is due to the abundance of micropores, as a fingerprint of hydrothermal alteration (Worden *et al.* 1990). They never display cross-hatched twinning, at least at the scale of optical microscopy. The core zone of most of the large crystals of primary albite

is decorated with small "droplets" of quartz. These early albite crystals show bent twin lamellae and deformation-induced twinning. Quartz commonly shows undulose extinction. Primary muscovite, scarce in discrete centimetric plates, seems at equilibrium with both primary feldspars. Most of the white mica occurs as small secondary anhedral flakes growing at the expense of the primary Li-aluminosilicate phases or along fractures.

Spodumene occurs as euhedral to subhedral crystals, with a predominant (100) and subordinate (110) development of the prism zone. It is mainly devoid of any mineral inclusions, suggesting that it precipitated quite early in the sequence. The simple twin (100) is common. Also present are irregularly shaped poikilitic crystals containing sparse blebs of quartz. Petalite was only identified in thin section. It follows spodumene as the stable Li-aluminosilicate (Fig. 3). Spodumene is in some cases penetrated, but not replaced by petalite along cracks or twin planes. Petalite is partly altered along grain boundaries to a brownish aggregate of microcrystals of eucryptite (see below). At Veral, needles of petalite, together with euhedral quartz, fill angular voids

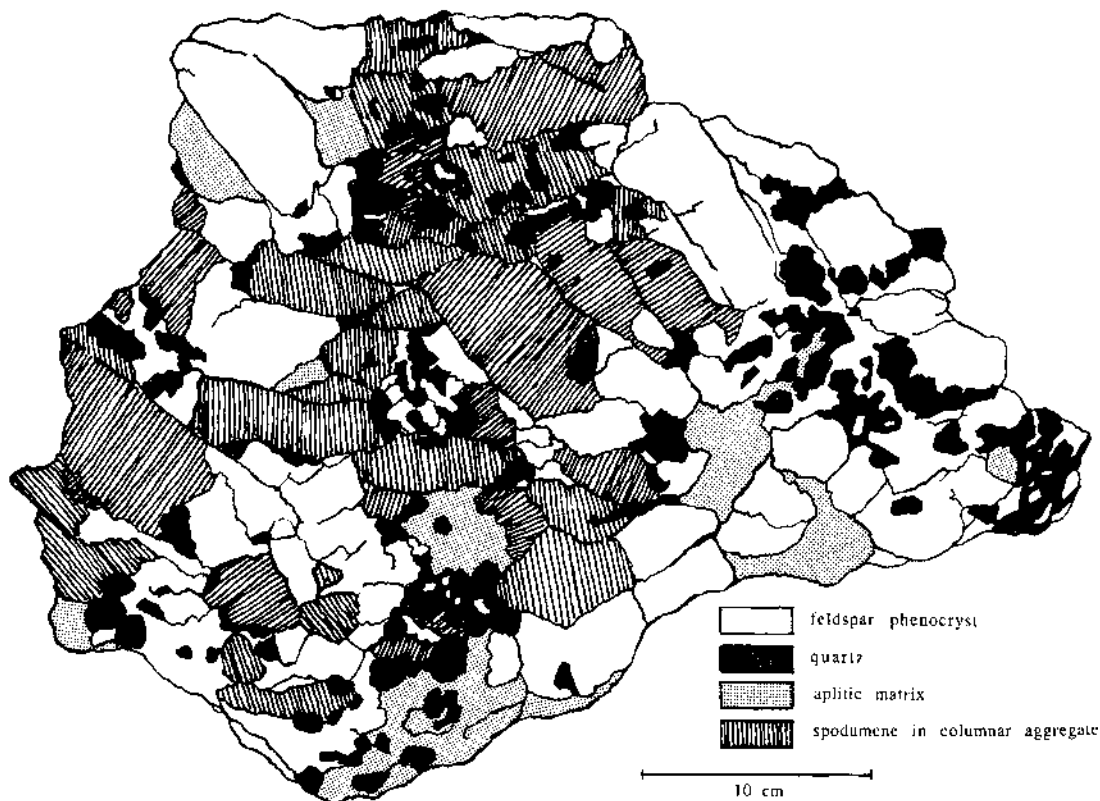


FIG. 2. Sketch of the macroscopic aspect of a strongly mineralized sample from Veral.

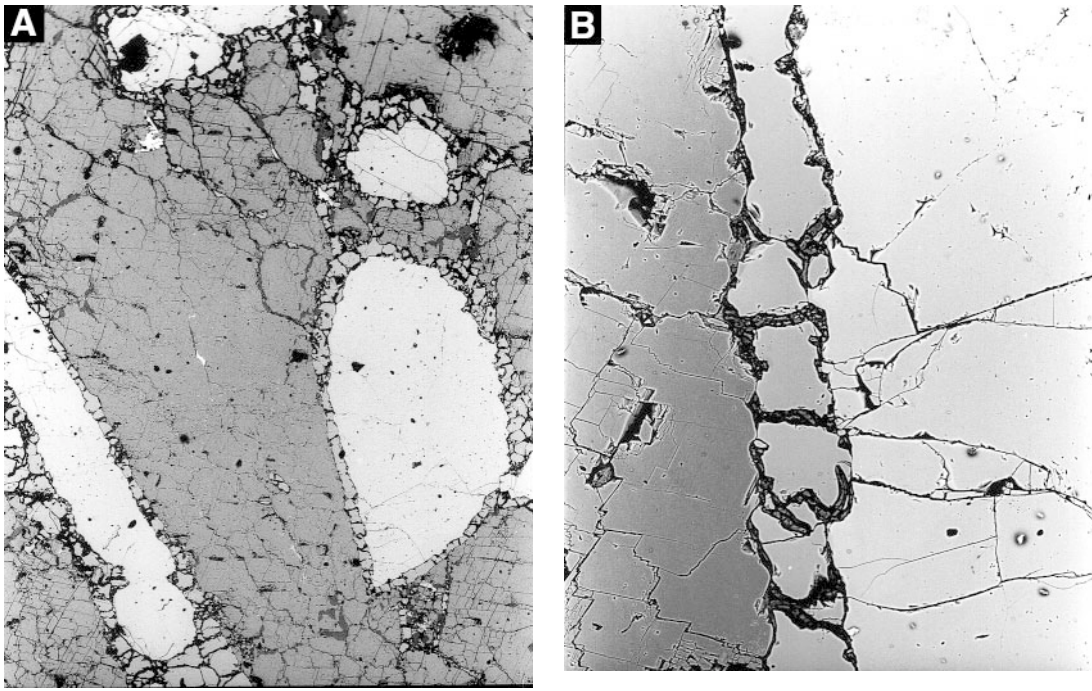


FIG. 3. Back-scattered electron (BSE) image showing Z-contrast between spodumene laths (grey) coated by polycrystalline petalite (light grey) against quartz (white) (A). Enlargement showing eucryptite in cracks cross-cutting petalite (B). Adagio pegmatite. Width of field of view: 2.4 mm in a, and 335  $\mu\text{m}$  in b.

among a meshwork of euhedral laths of spodumene (Fig. 4). Such a textural relationship shows that when the main generation of quartz precipitated, the medium was still saturated with Li–Al–silicate-forming components at P–T conditions in the field of stability of petalite. Spodumene and petalite develop a bright golden yellow and a deep dark blue cathodoluminescence, respectively (Görz *et al.* 1970), whereas quartz remains dark. Montebasite, which seems interstitial, is sporadically encountered as isolated, heavily altered grains with remnants of polysynthetic twinning.

The intimately mixed aplitic matrix may present a poorly developed banding defined by a rough variation in grain size, which signifies that the matrix is depositional and not replacive in origin. Na-rich plagioclase is the predominant (or only) feldspar present, with only occasional tapered phenocrysts of turbid K-feldspar. Quartz is not a dominant phase. Muscovite, as isolated flakes, together with rare grains of apatite, is subordinate.

#### Hydrothermal alteration

Widespread replacements show definite and consistently developed sequences, with selective corrosion leading up to complete replacement of spodumene by

albite ( $\pm$  muscovite), and of petalite by K-feldspar and eucryptite.

Albite is the major product of destabilization of spodumene. Remnants of spodumene in crystallographic continuity are embedded in medium-grained clear albite, which is surrounded by a fine-grained intergrowth of secondary K-feldspar + muscovite  $\pm$  eucryptite (Fig. 5). Albite may accumulate, in association with secondary K-feldspar, both with a branching habit. Part of this albite is subsequently altered to crystallographically oriented strings of white mica. In some cases, spodumene is invaded by radiating thin flakes of muscovite. In one case (ADG), euhedral vuggy prisms of spodumene in a large (decimetric) open cavity have been totally converted to a pale green, soft, waxy pseudomorph of nearly pure fine-grained white mica. This material is very similar to that described as “rotten spodumene” by Graham (1975). Mica flakes occur optically parallel to the three orientations (100), (110) and (110) of the original spodumene. Relations between both minerals are structurally controlled by a topotactic mechanism. Li was nearly completely leached out during this replacement: 7.23 and 0.13 wt%  $\text{Li}_2\text{O}$  remain in spodumene and pseudomorphic white mica, respectively.

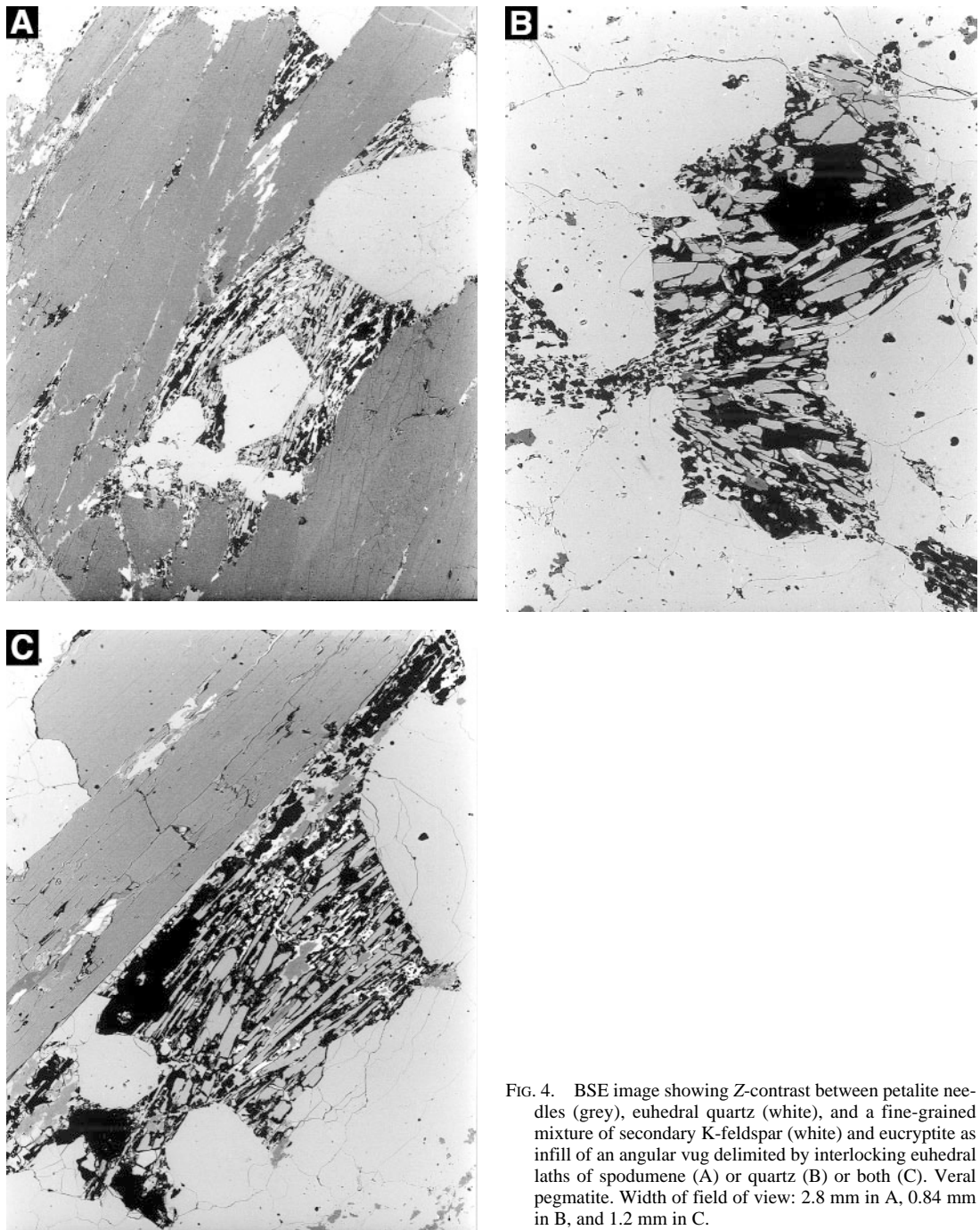


FIG. 4. BSE image showing Z-contrast between petalite needles (grey), euhedral quartz (white), and a fine-grained mixture of secondary K-feldspar (white) and eucryptite as infill of an angular vug delimited by interlocking euhedral laths of spodumene (A) or quartz (B) or both (C). Veral pegmatite. Width of field of view: 2.8 mm in A, 0.84 mm in B, and 1.2 mm in C.

Secondary K-feldspar is ubiquitous, in cross-cutting veinlets, alone or together with albite, or grown at the expense of petalite. It is invariably very turbid, and lacks

the occurrence of either distinctive grid twinning or albite exsolution. It is very difficult to discriminate between eucryptite and secondary K-feldspar under the

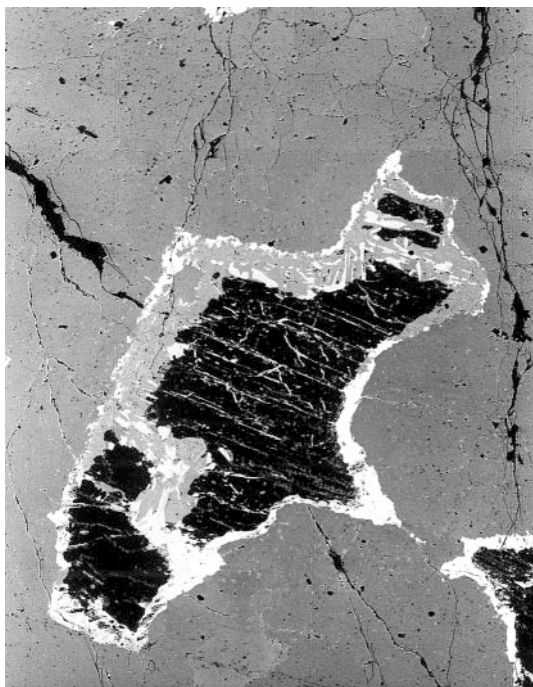


FIG. 5. BSE image showing Z-contrast between remnants of a spodumene crystal (black) replaced by albite (medium grey), blades of muscovite and a continuous rim of secondary K-feldspar (both white) with subordinate eucryptite (also black) Adagoi pegmatite. Width of field of view: 2.4 mm.

microscope, because both have a very turbid appearance, seem more or less contemporaneous, and generally are closely associated. The identification of eucryptite was very difficult. Eucryptite was firstly identified by its pale pinkish cream fluorescence in short-wave ultraviolet light (Mrose 1953, Hurlbut 1962); the observations were made with a microscope equipped with a UV (about 365 nm) source (Fig. 6). At high magnification, fluorescent eucryptite presents a low degree of crystallinity at a submicrometer scale. It is intimately mixed with amoeboid quartz, an Al-dominant phosphate, apatite and Ab grains in an alveolar mush-like mixture. Because of the poor resolution at a magnification of  $\times 40$ , the UV fluorescence seems to be homogeneous even though eucryptite is far from being the dominant phase in the mixture replacing petalite. Use of laser ablation – optical emission spectroscopy (Fabre 2000) confirms the occurrence of Li in such a mixture.

A Raman investigation conducted on the three Li-aluminosilicates give very good conclusions for spodumene and petalite, but disappointing results, because of the strong fluorescence, for eucryptite (Fig. 7), even though, contrary to spodumene and petalite, eucryptite

does not present any visible cathodoluminescence emission. Si/Al stoichiometry from EDS point-analyses confirm the coexistence of the three aluminosilicates at the thin-section scale (Fig. 8).

A quite similar sequence of alteration, but at a larger scale, involving the assemblages eucryptite + albite  $\pm$  K-feldspar and albite + muscovite, has been documented from many Li-rich pegmatites elsewhere (London & Burt 1982a). These subsolidus assemblages correspond to a  $\text{Na}^+$ -for- $\text{Li}^+$  ion-exchange reaction [spodumene +  $\text{Na}^+$  = eucryptite + Ab +  $\text{Li}^+$ ], followed by influx of  $\text{K}^+$  (growth of microcline) and  $\text{H}^+$  metasomatism (growth of muscovite). Therefore, subsolidus conditions were sufficiently alkaline to stabilize eucryptite + Ab or eucryptite + K-feldspar, and then later, relatively acid to form secondary mica (Montaya & Hemley 1975). During these episodes of alteration, Li was removed from the primary pegmatite assemblage, partially trapped in secondary eucryptite or leached out of the system and expelled toward the host rocks. Silica is also leached out. A slight increase of Li and Si contents in adjacent micaceous schists confirms our inference. Quartz is largely dominant in the final assemblage, as euhedral crystals or in aggregates with sutured joints and an undulose extinction.

Some of the samples studied are heavily altered, with only small remnants of spodumene in a very fine-grained, spongy mush of secondary minerals. These secondary phases, where phosphates of various compositions dominate, have not been fully characterized because of their small size and intimate intergrowth.

Tiny vugs are commonly encountered throughout the aplitic matrix. They probably result from the partial dissolution of albite by a free fluid phase collected as discrete bubbles along grain boundaries. That fluid mainly precipitated quartz, but also K-feldspar and eucryptite lining these vugs. Red brown sphalerite, with sparse inclusions of galena, occurs sporadically in interstices or associated with secondary quartz as an infilling of vugs.

A sequence of crystallization (Fig. 9) is tentatively established from the mutual relations among all the major and secondary mineral phases. The mineral sequence depicted represents the most complete paragenetic succession, even though the relative importance of one hydrothermal phase or the other differs widely from one sample to another, even in a given aplite-pegmatite body.

## DISCUSSION

Lithium, if present in a crystallizing system, does not behave as a typical alkali element (Heier & Billings 1970). It is not incorporated into the structure of the common felsic rock-forming minerals. Rather, the concentration of Li builds up progressively in the evolving closed pegmatite system, and reaches a level sufficient to trigger the crystallization of a Li-bearing phase. Where F is available, Li-bearing micas may be formed.

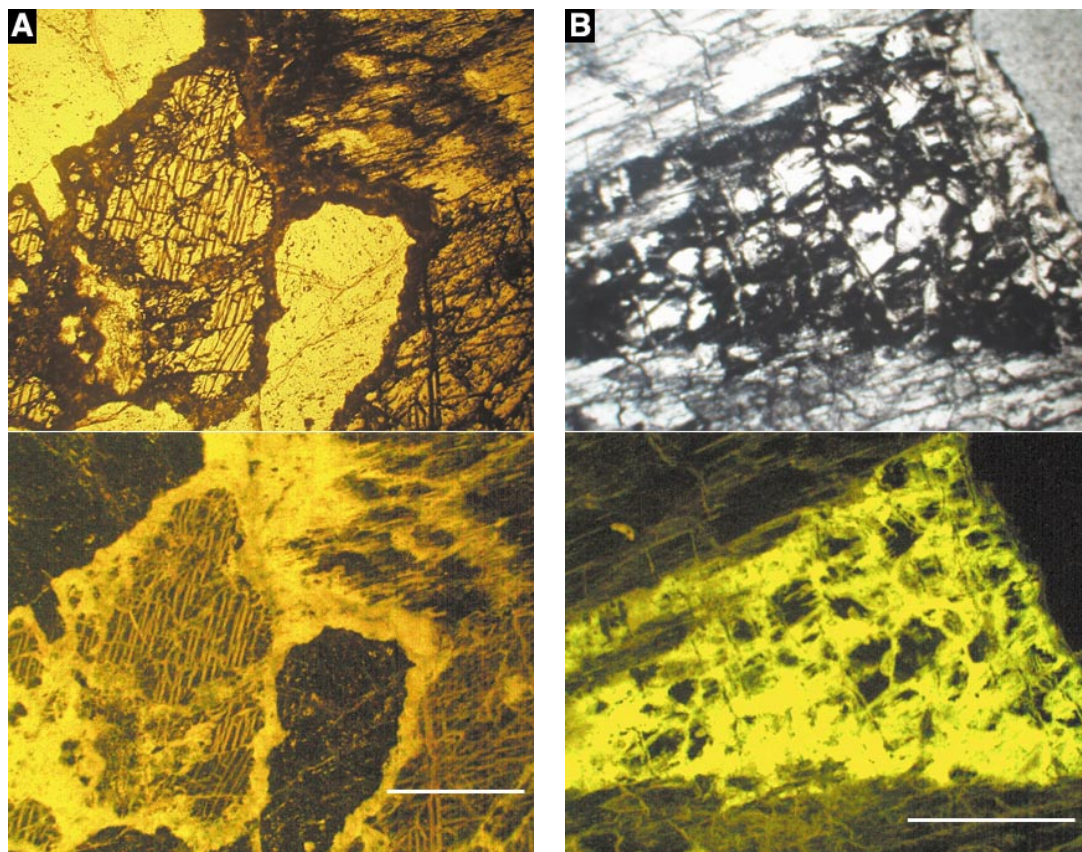
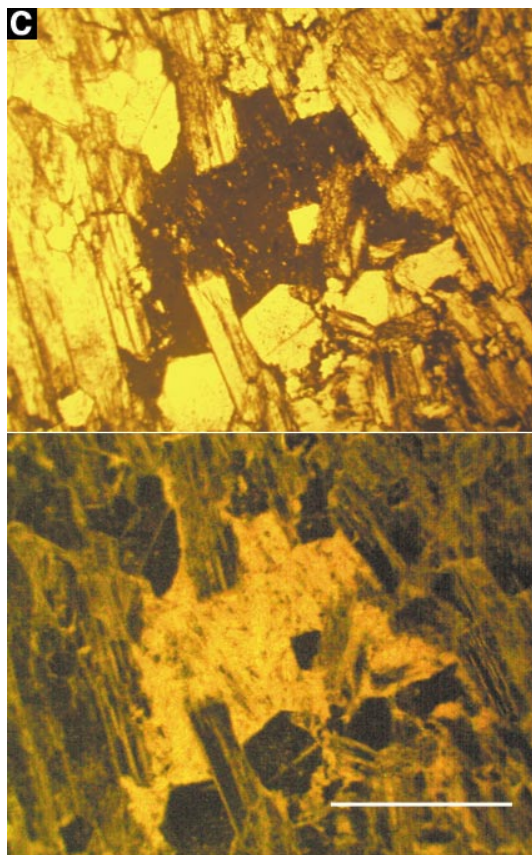


Fig. 6. Aspects of luminescence of eucryptite with UV light (natural and UV light doublets; scale bar: 1 mm). A. Relict spodumene embedded in fine-grained eucryptite derived from petalite. B. Eucryptite in cracks of vuggy petalite. C. Mush of eucryptite and K-feldspar around petalite needles in a void delimited by euhedral blades of spodumene (see Fig. 4A).

So, it largely behaves incompatibly. The starting material has roughly a granitic composition. Thermal and compositional inhomogeneities inside the crystallizing melt are generally assumed in huge, zoned pegmatite bodies (Jahns 1982, Webber *et al.* 1999), and the degree of undercooling of the melt dominates the kinetics of crystal nucleation and growth (London 1992). The occurrence of cavities delineated by euhedral laths of spodumene and of a few large vugs with free-standing euhedral crystals of spodumene suggests the presence of a separate fluid phase which, as experimentally demonstrated by London *et al.* (1989), will be only active at the last stage of pegmatite consolidation. In the ADG pegmatite, spodumene laths are wholly jacketed by a continuous thin coating of polycrystalline petalite in contact with quartz (Fig. 3). The stability field of the more siliceous petalite could be reached through a sudden drop in confining pressure, leading to the exsolution of an orthomagmatic hydrothermal fluid phase. An in-

crease of  $\mu\text{SiO}_2$  in this fluid would be likely (Stewart 1978). Both quartz- and feldspar-making components will be transferred into this fluid, and constitute, together with needle-like petalite, the infill of small scattered vugs, as present in samples of the Veral body (Fig. 4). The mutual relationships spodumene–petalite (Fig. 3) suggest that petalite precipitates from a thin film along the spodumene–fluid (silica-rich) interface. The fluid acting as a source of components for the crystallization of petalite was saturated with respect to this phase, and the spodumene was preserved metastably from dissolution. Stewart (1978) suggested that up to 0.64 wt% petalite can be dissolved in an aqueous vapour at 575°C, which is a normal consequence of closed-system subsolidus evolution of the pegmatite. The addition of silica in the fluid is also required to resaturate the rock with respect to petalite. Secondary quartz precipitates as vug infill or large interstitial aggregates (possibly pools of a silica-rich fluid).





The relatively small size of most of the aplite–pegmatite dykes points to a relatively rapid rate of cooling down to the metamorphic isotherms. A model of vigorous convection between melt and fluid, as proposed by Burnham & Nekvasil (1986) to explain the segregation of some particular lithophile element in a pegmatitic system, will be unlikely because of the narrow geometry and structural homogeneity of these Portuguese aplite–pegmatite dykes. A thermal gradient inside the body of pegmatite-forming melt, with Na preferentially enriched into the hotter (lower?) portions and K into the cooler (upper?) portions of the system, as suggested by the experimental results of Orville (1963), the conclusions of Jahns & Burnham (1969), and many pegmatite occurrences worldwide (Webber *et al.* 1999), contradicts our field observations; rather, an aplitic (mainly albitic) matrix seems to cement the megacrystic part (mainly K-feldspar) of the pegmatite paragenesis.

#### *Disequilibrium at the magmatic stage*

The pegmatite-forming magma, whatever its status, achieves saturation in a Li–aluminosilicate in the stabil-

ity field of spodumene. This condition is reached late in the main course of crystallization, after the precipitation of the feldspars. Petalite follows spodumene, but because of the lack of any apparent corrosion, spodumene remains (stably or metastably). The isochemical replacement of petalite by spodumene + 2 quartz (referred as “squi”), which is commonly observed in many Li-rich pegmatites (Hensen 1967, Černý & Ferguson 1972, Rossovskiy & Matrosov 1974, Gomes & Nunes 1990) has no relevance in our system. Chemical compositions of reliable bulk samples from the three aplite–pegmatite dykes investigated are not available, but partial analyses obtained from core sections at ALJ give 1.55 wt% Li<sub>2</sub>O on average and as high as 2.15 wt% (Lima *et al.* 1997). Bulk compositions of three pegmatitic (coarse-grained) fractions obtained by channel-sampling across some spodumene-bearing aplite–pegmatite dykes from the western part of the CDB pegmatite belt are available for comparison (samples CHN in Table 1; Charoy *et al.* 1992). Petalite and hydrothermal alteration of feldspars are lacking in these occurrences. The Li<sub>2</sub>O content varies from 1.35 up to 2.76 wt%. However, because of the selective sampling, such high contents cannot be representative of the initial pegmatite-forming melt as a whole. Stewart (1978) convincingly demonstrated, from experiments and reliable bulk compositions of pegmatites, that the Li content of many Li-rich pegmatites, representative of the lowest-temperature residual melt, clusters closely around 1.5 wt% Li<sub>2</sub>O

TABLE 1. COMPOSITION OF SOME SPODUMENE-BEARING PEGMATITE–APLITE BODIES FROM THE COVAS DE BARROSO DISTRICT, PORTUGAL

|                                 | CHN 5 | CHN 37 | CHN 42 | Pegm* | Harding |
|---------------------------------|-------|--------|--------|-------|---------|
| SiO <sub>2</sub> wt.%           | 73.15 | 76.06  | 78.34  | 74.19 | 75.24   |
| TiO <sub>2</sub>                | tr.   | tr.    | tr.    | 0.03  | 0.05    |
| Al <sub>2</sub> O <sub>3</sub>  | 16.14 | 16.56  | 16.60  | 14.79 | 14.42   |
| Fe <sub>2</sub> O <sub>3t</sub> | 0.81  | tr.    | tr.    | 0.68  | 0.62    |
| MnO                             | 0.04  | 0.02   | 0.04   | 0.05  | 0.18    |
| MgO                             | 0.15  | tr.    | tr.    | 0.07  | 0.01    |
| CaO                             | 0.19  | tr.    | tr.    | 0.12  | 0.20    |
| Na <sub>2</sub> O               | 2.45  | 2.31   | 0.56   | 4.26  | 4.23    |
| K <sub>2</sub> O                | 3.54  | 2.07   | 1.08   | 4.00  | 2.74    |
| P <sub>2</sub> O <sub>5</sub>   | 0.40  | 0.39   | 0.16   | 0.26  | 0.13    |
| F                               | 0.03  | 0.04   | 0.02   | 0.13  | 0.64    |
| LOI                             | 2.12  | 1.53   | 1.89   | 1.08  | n.d.    |
| O=F                             | 0.01  | 0.02   | 0.01   | 0.06  | 0.27    |
| total                           | 99.01 | 98.96  | 98.68  | 98.86 | 98.19   |
| Rb ppm                          | 770   | 370    | 191    | 388   | 1737    |
| Li                              | 6270  | 8900   | 12800  | 78    | 3033    |
| ASI                             | 1.25  | 1.32   | 1.44   | 1.28  | 1.16    |

Composition of some spodumene-bearing pegmatite–aplite bodies from the CDB district (Charoy *et al.* 1992); comparison with the chemical composition of the Harding pegmatite (Burnham & Nekvasil 1986). Pegm\*: pegmatite–aplite bodies from the nearby (two-mica granites (average of 6 samples). Li<sub>2</sub>O was included in the denominator of the expression for ASI (the Al saturation index). This had the approximate effect of removing the Li and Al components of spodumene

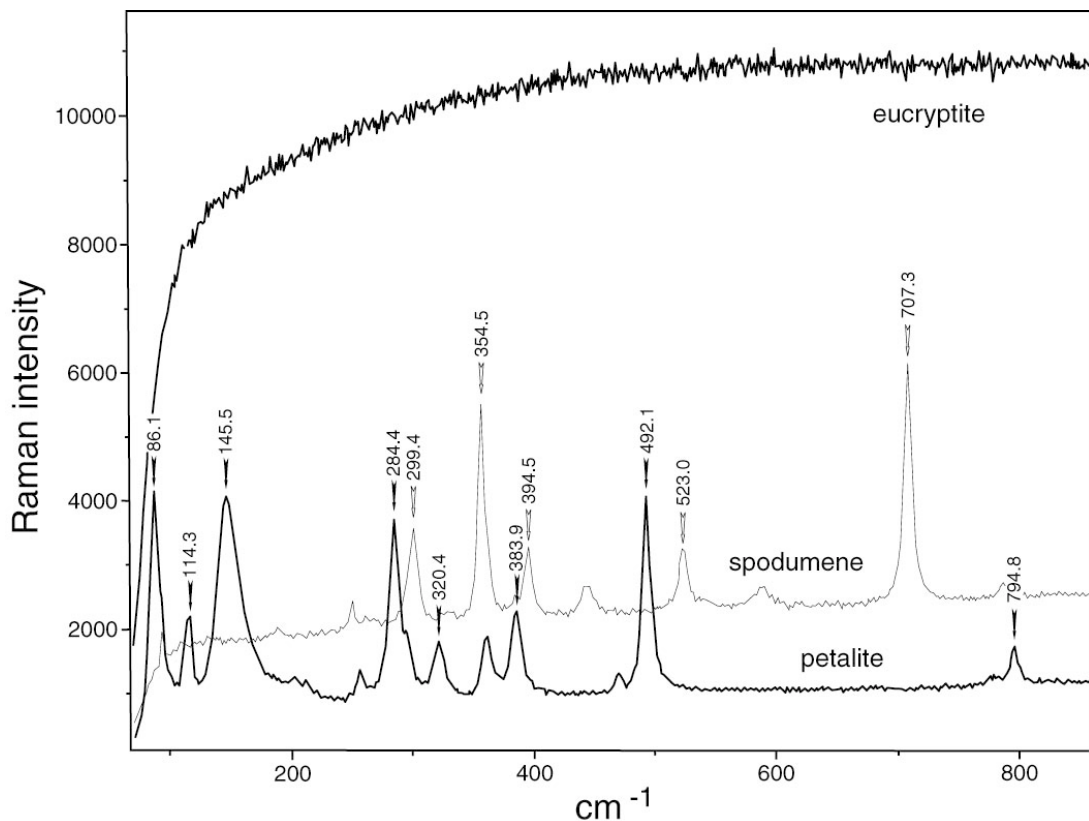


FIG. 7. Raman spectra of the three lithium aluminosilicates. Spectrometer: Labram DILOR (ORIBA). Analytical conditions: excitation line: HeNe laser, 632.817 nm (15 mW); grating: 1800 lines; slit: 300  $\mu\text{m}$  (G2R, UHP, Université de Nancy, Th. Lhomme, analyst).

(corresponding to about 20% spodumene), with 2.2 wt% claimed to be the upper limit of  $\text{Li}_2\text{O}$  that can accumulate in a melt. The aplitic portions, intimately mixed and genetically related with the pegmatitic fraction, have drastically lower Li contents (0.10 wt%  $\text{Li}_2\text{O}$ , on average). Therefore, it is obvious that Li in the initial melt was selectively partitioned into the pegmatitic, K-rich differentiates, in contrast to the aplitic, Na-rich segregations. On the other hand, Li is absent in pegmatites (Pegm\* in Table 1) encountered within the nearby two-mica granites.

#### *Disequilibrium at the hydrothermal stage*

Hydrothermal metasomatic replacement of pre-existing minerals implies the attainment of fluid saturation. The sporadic development of alteration within a given pegmatite, and even within a single thin section, signifies that these replacements are not produced by retrograde metamorphism but are indicators of changes in the chemistry of hydrothermal fluids. Coexistence of

heavily transformed and unreacted spodumene crystals at the thin-section scale can be explained either by kinetic barriers, inhomogeneity in fluid percolation, or by sealing of fractures and channelways due to the relatively larger molar volume of the alteration assemblage (London & Burt 1982a).

The first stage of subsolidus metasomatic alteration is usually alkaline (London & Burt 1982b, Burt & London 1982), followed by a weakly acid and potassic stage ("sericitic" alteration). Assuming a closed system, the total budget of Li in the fluid–mineral system should be constant. More and more Li will go into solution as the replacement of Li-bearing minerals by albite and K-feldspar progresses (Wood & Williams-Jones 1993). Therefore, both Na/Li and K/Li in the fluid generally will decrease with falling temperature. Replacement of spodumene (and eucryptite) by feldspars consumes silica, whereas the replacement of petalite liberates silica. As such, their replacement will not be contemporaneous but complementary:

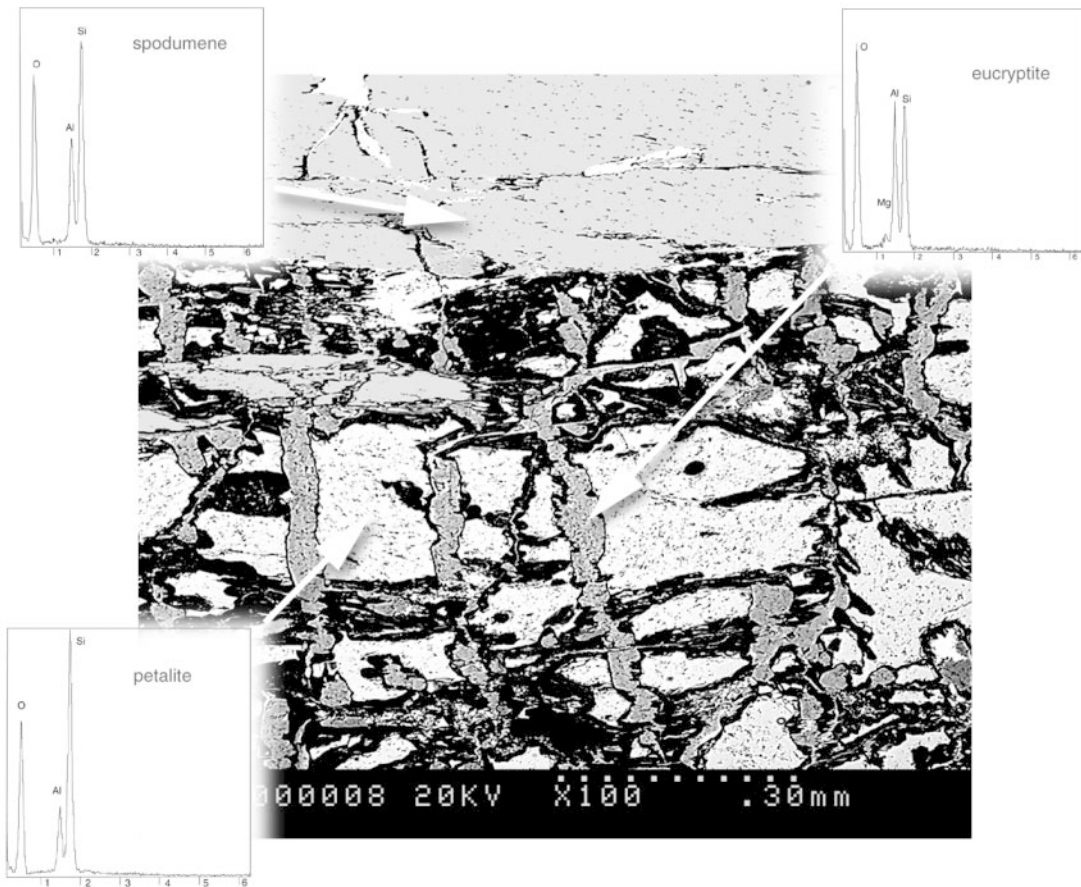
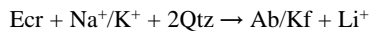
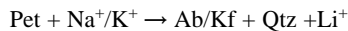
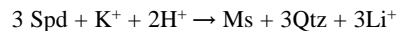
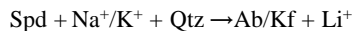


FIG. 8. BSE image illustrating the three coexisting Li aluminosilicates. At the top is a grain of euhedral marginal spodumene; medium gray: eucryptite as infill of fractures in petalite (white). Respective EDS spectra show the difference in Si/Al stoichiometry for the three phases. (Service commun de microanalyse, UHP Univ. de Nancy, A. Kohler, analyst). This microphotograph is an enlargement of Figure 6b.



According to the reaction  $\text{Spd} \rightarrow \text{Ecr} + \text{Qtz}$ , spodumene, eucryptite and quartz cannot be stable together, as is clear from the isobaric–isothermal  $\mu\text{Na-Li}_1 - \mu\text{SiO}_2$  diagram of Burt & London (1982). Whether spodumene breaks down to Ab or to Ecr + Ab depends primarily on the activity of silica within and around the crystals of spodumene (Rossovskiy 1971). Also, the formation of pseudomorphic mica in spodumene is enhanced by the local lowering of silica activity, according to:

However, the completeness of replacement of spodumene by white mica indicates that spodumene undergoing alteration does not buffer the cation-exchange potentials in the fluid, at least at that scale.

Gordiyenko *et al.* (1988) speculated about the chemical conditions necessary for the equilibrium Spd–Ms–Ab–Kfs (400°C, 100 MPa) present as aggregates in the more differentiated parts of many rare-metal pegmatites. According to their findings, spodumene grew hydrothermally from K-feldspar and was nearly always associated with albite. Spodumene and muscovite are more or less exclusive. These authors used four variables to compute the stability fields of the different minerals:  $\log[\text{K}^+]$ ,  $\log[\text{Na}^+]$ ,  $\log[\text{Li}^+]$  and pH. They apparently

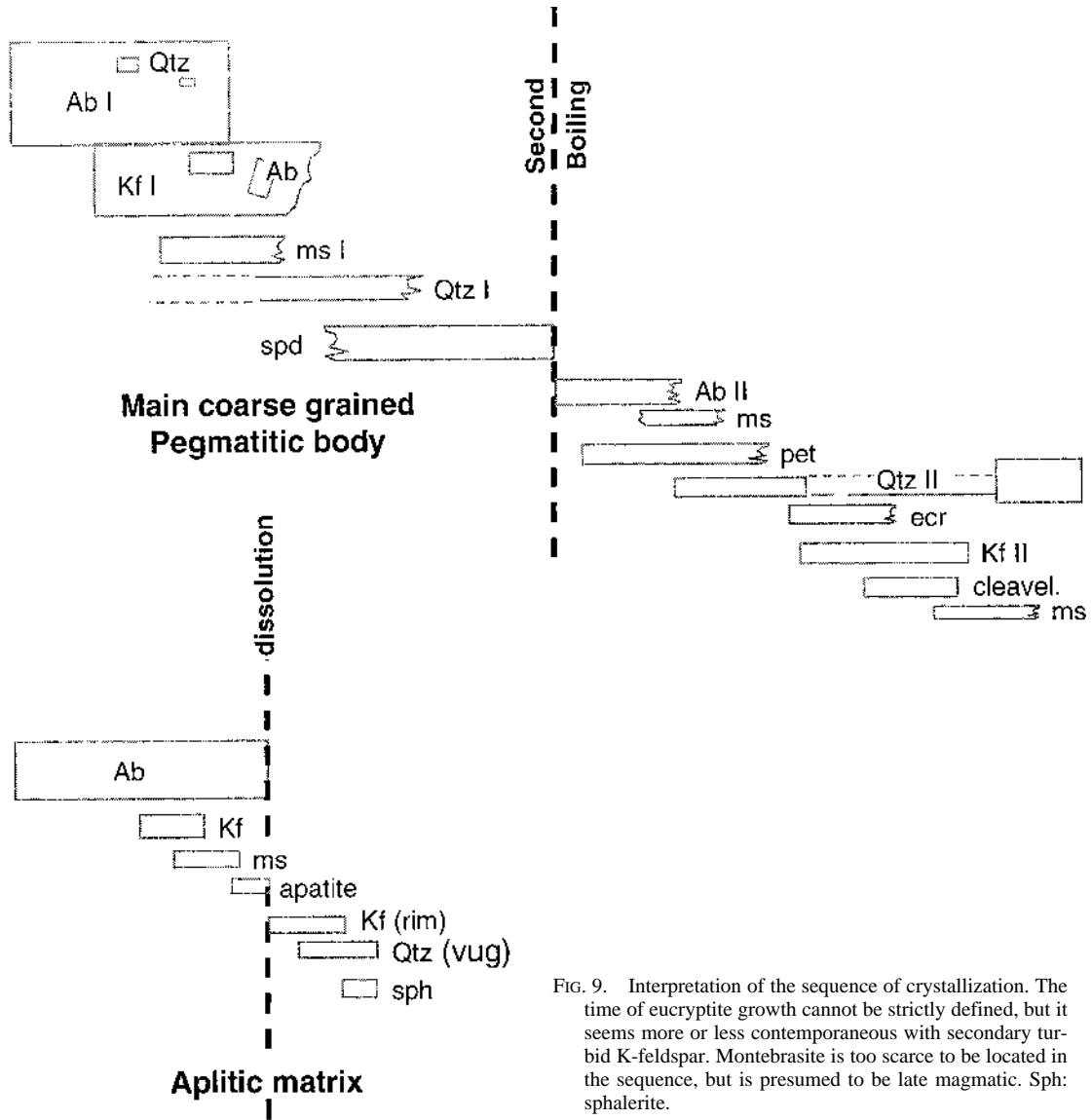


FIG. 9. Interpretation of the sequence of crystallization. The time of eucryptite growth cannot be strictly defined, but it seems more or less contemporaneous with secondary turbid K-feldspar. Montebasite is too scarce to be located in the sequence, but is presumed to be late magmatic. Sph: sphalerite.

ignored the relevant work of London (1984) about Li-aluminosilicate stabilities: in fact, petalite should be stable in place of spodumene at their referred physical conditions. Alkalinity of the medium, more than Li activity, should be of prime importance for the spodumene–muscovite competition, acidic for muscovite and more alkaline ( $\text{pH} > 6$ ) for spodumene. These results contradict their analytical data from fluid inclusion leachates on quartz from quartz–spodumene aggregates: Li is very minor, with Na/Li 8 to 17, whereas this ratio is found close to unity for comparable

experimental conditions at equilibrium (Sebastian & Lagache 1991, Lagache & Sebastian 1991).

Equilibrium boundaries for exchange reactions between an alkaline solution, feldspars and Li-aluminosilicates were computed by Wood & Williams-Jones (1993) between 100 and 700°C at different pressures. Assuming equilibrium among Ecr, Qtz, Ab and Kfs, K/Li and Na/Li activity ratios can be estimated (Fig. 10): K/Li = 0.01 and Na/Li = 0.18 for 200°C and 100 MPa. With these conditions, a solution (taken to be ideal) with 2 molal total alkalis in equilibrium with the above as-

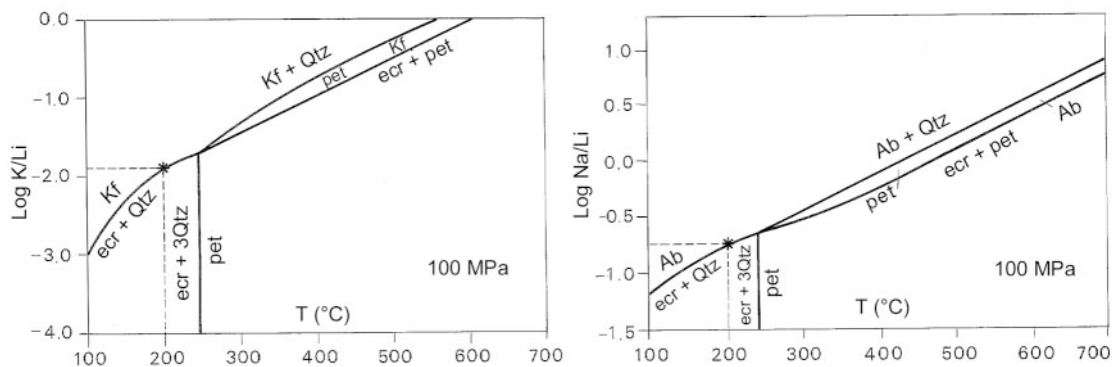


FIG. 10. Log activity (Na or K/Li) versus temperature at 100 MPa; activities can be computed from the equilibrium albite/(K-feldspar) – eucryptite – quartz at 200°C (redrawn from Wood & Williams-Jones 1993).

semblage of minerals is predicted to have roughly the following distribution of concentrations: 1.68 molal Li, 0.30 molal Na and 0.02 molal K, also far from the experimental results of Lagache & Sebastian (1991). Such an assessment confirms the disequilibrium likely in the system, with Li going into solution at the expense of the couple spodumene–petalite, whereas Na and K were continuously extracted from the solution to contribute to new feldspars. Fluids during such metasomatic processes are always out of equilibrium with their environment (London 1990); their Li content will increase dramatically with decreasing temperature (Wood & Williams-Jones 1993), and such fluids will be expected to invade the pegmatite envelope.

#### *P–T conditions*

Petalite and spodumene are antithetic in terms of P and T: the appearance of one in place of the other is not a function of composition of the medium, but mainly depends on externally imposed P–T conditions, with petalite as the high-T, low-P equivalent of spodumene in Li-rich pegmatites (Stewart 1978). Stability relations among the lithium aluminosilicates for quartz-saturated bulk compositions are shown in the Li–Al silicate grid proposed by London (1984), with the moderate- to low-T portion of the system directly applicable to the petrogenesis of Li-rich pegmatites (Fig. 10). The shallow P–T slope of the univariant reaction  $\text{Pet} \rightarrow \text{Spd}$  signifies that petalite–spodumene relations are more dependent on P than on T. Spodumene will be stable only at P above 170 MPa (the  $\text{Qtz} + \text{Pet} + \text{Spd} + \text{Ecr}$  invariant assemblage), which precludes its appearance in shallow, low-P environments. At magmatic temperatures of 500 to 700°C, pegmatites in which spodumene is the primary Li-aluminosilicate are constrained to crystallization pressures in the range of 300 to 400 MPa (London

1990). Under equilibrium conditions, petalite will be stable between 550–680°C at 200 MPa and 635–680°C at 400 MPa. Below both minimum temperatures, petalite will break down to the fine-grained  $\text{Spd} + \text{Qtz}$  intergrowth (squi). On the other hand, the stability field of  $\text{Ecr} + \text{Qtz}$  is limited to low P and T, below about 320°C and 160 MPa (London 1984), and most of the eucryptite replacement after petalite (or spodumene) would be expected to occur during uplift at 100–200°C (Chakoumakos & Lumpkin 1990). Therefore, the mineralogical evolution developed in our Portuguese aplite–pegmatite bodies suggests that primary crystallization and subsequent retrograde alteration span a broad P–T interval, with retrograde alteration operating down to low-P and low-T conditions (Fig. 10).

Fluid inclusions provide a means of evaluating minimum P–T conditions and fluid compositions during consolidation of pegmatites in recording the history of late-magmatic fluids and their subsequent evolution. This is a significant focus of research for understanding pegmatite genesis. Results from the literature are strikingly variable, covering a wide range of P–T conditions and compositions: from 260 to 350 MPa and from 420 to 675°C (London 1985, Whitworth & Rankin 1989, Chakoumakos & Lumpkin 1990, Fuertes-Fuente & Martin-Izard 1998). A fluid-inclusion study (Doria *et al.* 1989) was performed on a few spodumene-bearing pegmatites from the CDB pegmatite belt; maximum conditions of crystallization of spodumene were constrained to 250–300 MPa and 475–530°C. Fluid inclusions are very common in spodumene of the three occurrences studied, and are apparently primary, with a common distribution parallel to the long axis of the host mineral. They are mainly complex three-phase and  $\text{CO}_2$ -bearing, with variable  $\text{CO}_2:\text{H}_2\text{O}$  ratios at room temperature. Daughter minerals (carbonates) may be present (Lima 2000). The persistent occurrence of  $\text{CO}_2$  in flu-

ids in many complex granitic pegmatites worldwide demonstrates that CO<sub>2</sub> plays a determining role in their evolution (see literature above).

Temperature and pressure experienced during the peak of metamorphism of the host rocks throughout the province (500°C, 300 to 350 MPa; 11 to 13 km depth, Guedes *et al.* 1997) provide an upper boundary for the pressure of emplacement and crystallization of the pegmatite-forming liquids. Muscovite can be stable below H<sub>2</sub>O saturation of the melt; its occurrence does not preclude any H<sub>2</sub>O saturation through the exsolution of an aqueous fluid. Consequently, the main part of the albite-pegmatite crystallizes in conditions of H<sub>2</sub>O undersaturation, as recently demonstrated by London *et al.* (1989). As discussed above, fluid saturation was reached once the main part of the pegmatite body had already crystallized. One may confidently infer that the main part of the exsolved aqueous fluid remained in the system. Pegmatite-induced alteration is not prevalent in the micaceous schists around the bodies studied, and there is apparently no mineralogical evidence of any metasomatic alteration. Nevertheless, there is a significant chemical interaction between the proximal host rocks and fluids derived from the pegmatites, because Li content (up to 1000 ppm Li, Lima *et al.* 1997) is three to five times the background in adjacent schists. Fine-grained intergranular eucryptite (as revealed in a cursory UV investigation) could be responsible for this exomorphic halo.

K-feldspar phenocrysts are well-ordered (low) microcline. As described earlier, such feldspar is not cross-hatched, and exsolution lamellae of albite are rare or absent in thin section. An X-ray powder-diffraction investigation conducted on a dozen of alkali feldspar phenocrysts (3 to 5% mole Ab, reflecting quite a low temperature of final equilibration) shows that all are fully ordered microcline (obliquity  $\approx$  0.85 to 0.90; computed  $t_{10} + t_{1m} = 1.00$ ). The sodic plagioclase that coexists with the microcline is close to the Ab end-member (An<sub>0-3</sub> by electron-microprobe analysis). These nearly pure end-members (Table 2) are in equilibrium and considered to have equilibrated at a subsolidus temperature by fluid-mediated recrystallization. Twinning was obliterated at a quite low temperature, below the temperature of the orthoclase-microcline transition (Černý & Macek 1972).

A fairly well constrained P-T path of crystallization spanning from magmatic to subsolidus conditions for these pegmatite bodies is shown in Figure 11.

### The pegmatite field as a whole

Geological mapping of pegmatite belts worldwide has, at least statistically, proven the existence of a regional compositional zoning, and the rare-element pegmatites outcrop farthest from the supposed parental granites (Černý 1991b, 1992, Norton & Redden 1990, Shearer *et al.* 1992, Fuertes-Fuente & Martin-Izard

1998). Li-rich pegmatites are certainly more numerous than known examples indicate in this Hercynian part of Portugal. Other occurrences are already known westward (Gomes & Nunes 1990), but with quite different phase relations: petalite is the early phase, and is affected by a subsequent "squi" breakdown, which signifies a different evolution in the pressure regime. The apparent dispersion of the already recognized Li-bearing pegmatite dykes in the CDB district (Fig. 1) does not provide convincing field evidence of any genetic relationship with the nearby, apparently more favorable, two-mica granites. The numerous pegmatitic differentiates within these two-mica granites (interior pegmatites) are Li-free (Pegm\* in Table 1), as routinely documented in most examples of pegmatite populations worldwide. However, there is a very different pattern among the mineralized pegmatite bodies, according to their loca-

TABLE 2. AVERAGE CHEMICAL COMPOSITIONS AND STRUCTURAL FORMULAE OF THE MAIN PRIMARY AND SECONDARY MINERAL PHASES, COVAS DE BARROSO SUITE

|                                | Kfs I<br>ADAG | Ab I<br>ALJ | Spd<br>ALJ | Pet<br>ADAG | Ms<br>ALJ | Mbs<br>VERAL | Kfs II<br>ADAG | Ab II<br>ALJ |
|--------------------------------|---------------|-------------|------------|-------------|-----------|--------------|----------------|--------------|
|                                | 2             | 1           | 1          | 2           | 1         |              | 2              | 3            |
| SiO <sub>2</sub> wt%           | 65.07         | 68.80       | 65.09      | 78.91       | 46.28     | -            | 64.95          | 68.19        |
| Al <sub>2</sub> O <sub>3</sub> | 18.41         | 19.40       | 27.20      | 16.75       | 37.19     | 35.07        | 18.40          | 20.27        |
| FeO*                           | 0.05          | -           | 0.23       | 0.05        | 0.47      | -            | 0.07           | -            |
| MnO                            | 0.10          | -           | 0.01       | 0.03        | -         | -            | -              | -            |
| MgO                            | 0.03          | -           | -          | -           | 0.01      | -            | 0.02           | 0.03         |
| CaO                            | 0.01          | 0.03        | -          | -           | 0.06      | -            | -              | 0.06         |
| Na <sub>2</sub> O              | 0.60          | 12.20       | 0.01       | 0.01        | 0.63      | 0.01         | 0.08           | 11.40        |
| K <sub>2</sub> O               | 15.86         | 0.13        | -          | -           | 10.72     | -            | 16.37          | 0.11         |
| P <sub>2</sub> O <sub>5</sub>  | -             | 0.21        | 0.06       | 0.05        | 0.09      | 49.75        | -              | 0.19         |
| Li <sub>2</sub> O              | n.d.          | n.d.        | 7.65       | 4.49        | n.d.      | 8.87         | n.d.           | n.d.         |
| F                              | -             | -           | -          | -           | -         | 0.40         | -              | -            |
| O=F                            | -             | -           | -          | -           | -         | 0.17         | -              | -            |
| Sum                            | 100.13        | 100.77      | 100.25     | 100.29      | 95.45     | 95.93        | 99.89          | 100.25       |
|                                | 32 O          | 32 O        | 24 O       | 20 O        | 22 O      | 5(O,OH,F)    | 32 O           | 32 O         |
| Si <i>apfu</i>                 | 11.99         | 12.59       | 8.06       | 8.03        | 6.13      | -            | 12.01          | 11.87        |
| Al                             | 4.01          | 4.18        | 3.86       | 2.01        | 5.79      | 1.01         | 4.01           | 4.15         |
| P                              | -             | 0.03        | 0.01       | -           | 0.01      | 1.03         | -              | 0.03         |
| Mg                             | 0.01          | -           | -          | -           | -         | -            | 0.01           | 0.01         |
| Fe                             | 0.01          | -           | 0.02       | 0.01        | 0.05      | -            | 0.01           | -            |
| Ca                             | -             | 0.01        | -          | -           | 0.01      | -            | -              | 0.01         |
| Na                             | 0.22          | 4.33        | -          | -           | 0.16      | -            | 0.02           | 4.04         |
| K                              | 3.72          | 0.02        | -          | -           | 1.81      | -            | 3.87           | 0.02         |
| Li                             | -             | -           | 3.80       | 1.83        | -         | 0.87         | -              | -            |
| F                              | -             | -           | -          | -           | -         | 0.04         | -              | -            |
| OH                             | -             | -           | -          | -           | -         | 0.96         | -              | -            |
| Or                             | 94            | 0.5         | -          | -           | -         | -            | 99             | 1            |
| Ab                             | 6             | 99          | -          | -           | -         | -            | 1              | 98           |
| An                             | -             | 0.5         | -          | -           | -         | -            | -              | 1            |

The quantitative electron-microprobe analyses were made with an automated Cameca SX50 microprobe housed at UHP - Université de Nancy I (Service commun de microanalyse). Operating conditions: 15 kV, beam current 5 nA, beam diameter 3 to 5 µm, and a counting time on peaks of 20 s. Li contents were measured *in situ* with a Cameca IMS 3f secondary-ion mass spectrometer at the CRPG (Nancy). A 0.5 nA O<sup>-</sup> primary beam at 10 kV was used. Secondary ions of Li and Si (Li and P for montebrasite) were analyzed at 800 or 2000 mass resolution. <sup>7</sup>Li/<sup>6</sup>Si and <sup>7</sup>Li/<sup>31</sup>P ratios were measured on the samples and mineral standards (spodumene and amblygonite). Note that Rb is quite low (1250 to 3000 ppm) in Kfs I and undetectable in Ab I. P<sub>2</sub>O<sub>5</sub> is low but significant in albite. Symbols: Kfs K-feldspar, Ab albite, Spd spodumene, Pet petalite, Ms muscovite, Mbs montebrasite, *apfu*: atoms per formula unit.

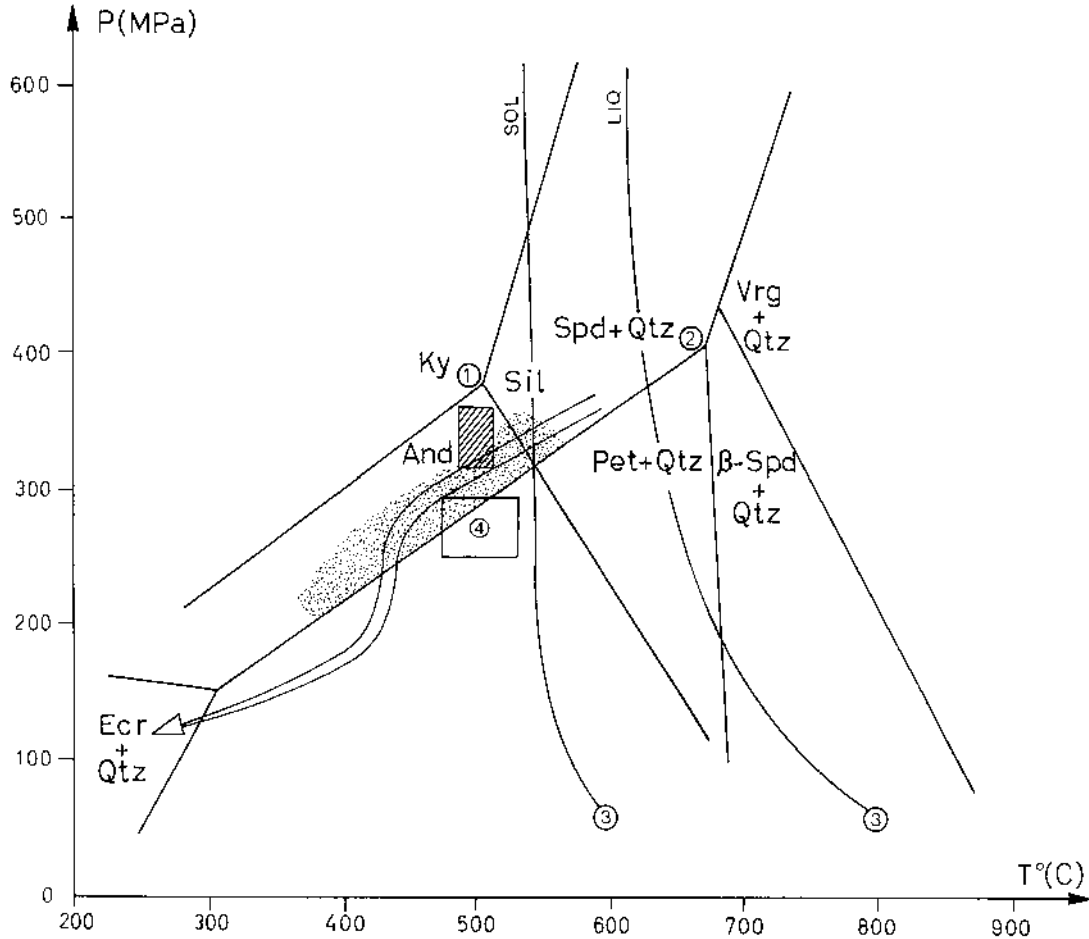


FIG. 11. Inferred pressure-temperature path (arrow) for the magmatic-hydrothermal crystallization of the aplite-pegmatite dykes. Features in the diagram: 1 the triple point for the aluminosilicates (Holdaway 1971), 2 the Li-Al silicate grid (London 1984), 3 the liquidus to solidus interval for the Harding pegmatite (Jahns 1982), 4 the maximum conditions for the crystallization of spodumene in the CDB pegmatite belt (Doria *et al.* 1989). The stippled area shows the probable P-T range for crystallization of the spodumene + quartz assemblage in Li-enriched granitic pegmatites (London & Burt 1982b). The hatched area shows the peak conditions of regional metamorphism.

tion within the CDB pegmatite belt. The western ones (CHN bodies) are free of petalite and alteration to feldspars (Charoy *et al.* 1992), whereas the eastern ones (this study) exhibit a more complex evolution: petalite is present, and there is widespread alteration to feldspars. Such a contrasted behavior suggests some direct link with the intrusion of post-tectonic (post-pegmatite) biotite granites to the East. A drop in pressure (spodumene to petalite) may be related to the system of NNE-SSW (Régua-Verin, inset in Fig. 1) sinistral faults developed close to the eastern part of the belt (Guedes *et al.* 1997). This fault system permitted the ascent of the magma that formed the biotite granite, with the consequent overprint

on the nearby older occurrences of pegmatite. It is not the case in the western part of the belt.

#### CONCLUSIONS

Aplite-pegmatite dykes of granitic composition are numerous in this Iberian part of the Hercynian orogeny, but only a very small percentage of them is Li-rich, with spodumene and, more rarely, petalite as primary phases. For the first time, the full sequence of the three Li-aluminosilicates spodumene, petalite and eucryptite, and their relative chronological relationships, are described in detail for some aplite-pegmatite dykes from northern

Portugal. The magmatic paragenesis in the pegmatitic portions is assumed to be albite + K-feldspar + quartz (minor) + muscovite (accessory) + spodumene (with a highly heterogeneous distribution), in contrast with the quite minor aplitic matrix, where albite is largely dominant and spodumene absent. Petalite follows spodumene as a result of a sudden drop in confining pressure (from lithostatic to hydrostatic?), probably contemporaneously with some Hercynian faulting and associated uplift of the chain, which generates a separate fluid phase. It seems likely that petalite precipitated directly from that fluid. Mirolitic cavities (as in Veral) constitute evidence of fluid saturation prior to the complete crystallization of the pegmatite-forming melt. The hydrothermal history of the pegmatite body began with the widespread but variable metasomatic replacement of the former Li-aluminosilicates, marginally or along cracks, mostly by albite, muscovite and K-feldspar, and by late eucryptite selectively at the expense of petalite, together with secondary phosphates. During this superimposed hydrothermal alteration, Li is progressively leached out of the system and dispersed into the surrounding metasedimentary units. The P-T path suggested for the evolution of these Portuguese Li-rich aplite-pegmatite bodies seems to be atypical with regard to most of the descriptions in the literature, because spodumene remains stable (or metastable) against petalite, contrary to what is generally encountered elsewhere.

#### ACKNOWLEDGEMENTS

P. Černý, R.F. Martin and an anonymous reviewer provided constructive and helpful comments. It is a real pleasure to acknowledge the guidance they gave us.

#### REFERENCES

- BRISBIN, W.C. (1986): Mechanics of pegmatite intrusion. *Am. Mineral.* **71**, 644-651.
- BURNHAM, C.W. & NEKVASIL, H. (1986): Equilibrium properties of granite pegmatite magmas. *Am. Mineral.* **71**, 239-263.
- BURT, D.M. & LONDON, D. (1982): Subsolidus equilibria. In *Granitic Pegmatites in Science and Industry* (P. Černý, ed.). *Mineral. Assoc. Can., Short Course Handbook* **8**, 329-346.
- CAMERON, E.N., JAHNS, R.H., MCNAIR, A.H. & PAGE, L.R. (1949): Internal structure of granitic pegmatites. *Econ. Geol., Monogr.* **2**.
- ČERNÝ, P. (1972): The Tanco pegmatite at Bernic Lake, Manitoba. VIII. Secondary minerals from the spodumene-rich zones. *Can. Mineral.* **11**, 714-728.
- \_\_\_\_\_ (1982): Petrogenesis of granite pegmatites. In *Granitic pegmatites in Science and Industry* (P. Černý, ed.). *Mineral. Assoc. Can., Short Course Handbook* **8**, 405-461.
- \_\_\_\_\_ (1991a): Rare-element granitic pegmatites. I. Anatomy and internal evolution of pegmatite deposits. *Geosci. Canada* **18**(2), 49-67.
- \_\_\_\_\_ (1991b): Rare-element granitic pegmatites. II. Regional to global environments and petrogenesis. *Geosci. Canada* **18**(2), 68-81.
- \_\_\_\_\_ (1992): Geochemical and petrogenetic features of mineralization in rare-element granitic pegmatites in the light of current research. *Appl. Geochem.* **7**, 393-416.
- \_\_\_\_\_ (1993): Fractionation in granite + rare-element pegmatite systems. Facts and fiction. In *Current Research in Geology Applied to Ore Deposits* (P. Fenoll Hach-Alf, J. Torres-Ruiz & F. Gervilla, eds.). *Second Bien. SGA Meeting (Granada), Abstr.*, 23-26.
- \_\_\_\_\_ & FERGUSON, R.B. (1972): The Tanco Pegmatite at Bernic Lake, Manitoba. IV. Petalite and spodumene relations. *Can. Mineral.* **11**, 660-678.
- \_\_\_\_\_ & MACEK, J. (1972): Petrology of potassium feldspars in two lithium-bearing pegmatites. In *The Feldspars* (W.S. MacKenzie & J. Zussman, eds). *Proc. NATO Adv. Study Inst.* Manchester Univ. Press, Manchester, U.K. (615-628).
- CHAKOUMAKOS, B.C. & LUMPKIN, G.R. (1990): Pressure-temperature constraints on the crystallization of the Harding pegmatite, Taos County, New Mexico. *Can. Mineral.* **28**, 287-298.
- CHAROY, B., LHOTE, F., DUSAUSOY, Y. & NORONHA, F. (1992): The crystal chemistry of spodumene in some granitic aplite-pegmatite of northern Portugal. *Can. Mineral.* **30**, 639-651.
- DORIA, A., CHAROY, B. & NORONHA, F. (1989): Fluid inclusion studies in spodumene-bearing aplite-pegmatite dykes of Covas de Barroso, northern Portugal. *ECROFIX* (London), **25** (abstr.).
- FABRE, C. (2000): Reconstitution chimique des paléofluides par spectrométrie d'émission optique couplée à l'ablation laser. Applications aux fluides alpins et aux fluides de bassins. Thèse de doctorat, Univ. de Nancy I, Nancy, France.
- FENN, P.M. (1986): On the origin of graphic granite. *Am. Mineral.* **71**, 325-330.
- FERREIRA, N., IGLESIAS, M., NORONHA, F., PEREIRA, E., RIBEIRO, A. & RIBEIRO, M.L. (1987): Granitoides da Zona Centro Iberica e seu enquadramento geodinamico. In *Geologia de los Granitoides y Rocas Asociadas del Macizo* (F. Bea *et al.*, eds.). Libro Homenaje a L.C. Garcia de Figuerola, Hespérico Editorial Rueda, Madrid, Spain (37-51).
- FUERTES-FUENTE, M. & MARTIN-IZARD, A. (1998): The Forcarei Sur rare-element granitic pegmatite field and its



- associated mineralization, Galicia, Spain. *Can. Mineral.* **36**, 303-325.
- GINSBURG, A.I. (1984): The geological condition of the location and the formation of granitic pegmatites. *Proc. 27th Int. Geol. Congress* **15**, 245-260.
- \_\_\_\_\_ & GUSHCHINA, N.S. (1954): Petalite from pegmatites of the eastern Transbaikali region. *Trudy Mineral. Muz., Akad. Nauk SSSR* **6**, 71-85 (in Russ.).
- GOMES, C.L. & NUNES, J.E.L. (1990): As paragénese correspondantes à mineralização litínifera do campo aplito-pegmatítico de Argá-Minho (Norte de Portugal). *Memorias e Noticias* **109**, 131-166.
- GORDIYENKO, V.V., ZHUKOVA, I.A. & PONOMAREVA, N.I. (1988): The physicochemical conditions of quartz–spodumene and quartz–muscovite aggregates in rare-metal granite pegmatites. *Int. Geol. Rev.* **30**, 53-61.
- GÖRZ, H., BHALLA, R.J.R.S.B. & WHITE, E.W. (1970): Detailed cathodoluminescence characterization of common silicates. In *Space Science Applications of Solid State Luminescence Phenomena* (J.N. Weber & E. White, eds). *Penn. State Univ., Mater. Res. Lab. Publ.* **70-101**, 62-70.
- GRAHAM, J. (1975): Some notes on  $\alpha$ -spodumene,  $\text{LiAlSi}_2\text{O}_6$ . *Am. Mineral.* **60**, 919-923.
- GUEDES, A., DORIA, A., NORONHA, F. & BOIRON, M.C. (1997): Fluid inclusion studies in Paleozoic C-rich meta-sedimentary rocks from northern Portugal. In *Proc. XIV ECROFI Conf.* (M.C. Boiron & J. Pironon, eds), 138-139.
- HEIER, K.S. & BILLINGS, G.K. (1970): Lithium. In *Handbook of Geochemistry II* (K.H. Wedepohl, ed.). Springer-Verlag, Berlin, Germany.
- HEINRICH, E.W. (1948): Pegmatites of Eight Mile Park, Fremont County, Colorado. *Am. Mineral.* **33**, 550-587.
- HENSEN, B.J. (1967): Mineralogy and petrography of some tin, lithium and beryllium bearing albite-pegmatites near Doade, Galicia, Spain. *Leidse Geol. Med.* **39**, 249-259.
- HOLDAWAY, M.J. (1971): Stability of andalusite and the aluminum silicate phase diagram. *Am. J. Sci.* **271**, 97-131.
- HURLBUT, C.S., JR. (1962): Eucryptite from Bikita, Southern Rhodesia. *Am. Mineral.* **47**, 557-561.
- JAHNS, R.H. (1982): Internal evolution of granitic pegmatites. In *Granitic Pegmatites in Science and Industry* (P. Černý, ed.). *Mineral. Assoc. Can., Short Course Handbook* **8**, 293-328.
- \_\_\_\_\_ & BURNHAM, C.W. (1969): Experimental studies of pegmatite genesis. I. A model for the derivation and crystallization of granitic pegmatites. *Econ. Geol.* **64**, 843-864.
- LAGACHE, M. & SEBASTIAN, A. (1991): Experimental study of Li-rich granitic pegmatites. II. Spodumene + albite + quartz equilibrium. *Am. Mineral.* **76**, 611-616.
- LIMA, A. (2000): *Estrutura mineralogia e génese dos filões aplitopegmatitos com espodumena da região de Barroso-Alvão*. Ph.D. thesis, Univ. Porto-INPL, Porto, Portugal.
- \_\_\_\_\_, FARINHA, J., PIRES, M., VIEGAS, L., CHAROY, B., NORONHA, F. & MARTINS, L. (1997): Prospeção de jazidas da lítio na região de Barroso-Alvão. *Actas X Semana de Geoquímica/IV Congresso de Geoquímica dos Países de Língua Portuguesa (Braga), Resumos*, 199-202.
- LONDON, D. (1984): Experimental phase equilibria in the system  $\text{LiAlSiO}_4\text{-SiO}_2\text{-H}_2\text{O}$ : a petrogenetic grid for lithium-rich pegmatites. *Am. Mineral.* **69**, 995-1004.
- \_\_\_\_\_ (1985): Origin and significance of inclusions in quartz: a cautionary example from the Tanco pegmatite, Manitoba. *Econ. Geol.* **80**, 1988-1995.
- \_\_\_\_\_ (1990): Internal differentiation of rare-element pegmatites; a synthesis of recent research. In *Ore-Bearing Granite Systems: Petrogenesis and Mineralizing Processes* (H.J. Stein & J.L. Hannah, eds). *Geol. Soc. Am., Spec. Pap.* **246**, 35-50.
- \_\_\_\_\_ (1992): The application of experimental petrology to the genesis and crystallization of granitic pegmatites. *Can. Mineral.* **30**, 499-540.
- \_\_\_\_\_ & BURT, D.M. (1982a): Alteration of spodumene, montebrasite and lithiophilite in pegmatites of the White Picacho district, Arizona. *Am. Mineral.* **67**, 97-113.
- \_\_\_\_\_ & \_\_\_\_\_ (1982b): Chemical models for lithium aluminosilicate stabilities in pegmatites and granites. *Am. Mineral.* **67**, 494-509.
- \_\_\_\_\_, MORGAN, G.B., VI & HERVIG, R.L. (1989). Vapor-undersaturated experiments with Macusanite glass +  $\text{H}_2\text{O}$  at 200 MPa, and the internal differentiation of granitic pegmatites. *Contrib. Mineral. Petrol.* **102**, 1-17.
- MONTAYA, J.W. & HEMLEY, J.J. (1975): Activity relations and stabilities in alkali feldspar and mica alteration reactions. *Econ. Geol.* **70**, 577-583.
- MROSE, M.E. (1953): The  $\alpha$ -eucryptite problem. *Am. Mineral.* **38**, 353 (abstr.).
- NORONHA, F., RAMOS, J.M.F., REBELO, J., RIBEIRO, A. & RIBEIRO, M.L. (1981): Essai de corrélation des phases de déformation hercyniennes dans le NW de la Péninsule Ibérique. *Leid. Geol. Meded.* **52**(1) 87-91.
- NORTON, J.J. (1983): Sequence of mineral assemblages in differentiated granitic pegmatites. *Econ. Geol.* **78**, 854-874.
- \_\_\_\_\_ & REDDEN, J.A. (1990): Relations of zoned pegmatites to other pegmatites, granite, and metamorphic rocks in the southern Black Hills, South Dakota. *Am. Mineral.* **75**, 631-655.
- ORVILLE, P.E. (1963): Alkali ion exchange between vapor and feldspar phases. *Am. J. Sci.* **261**, 201-237.

- RIBEIRO, A., ANTUNES, M.T., PORTUGAL FERREIRA, M., ROCHO, R.B., SOARES, A.F., ZBYSZEWSKI, G., MOITINHO DE ALMEIDA, F., DE CARVALHO, D. & MONTEIRO, J.H. (1979): Introduction à la géologie générale du Portugal. *Serv. Geol. Portugal*.
- ROSSOVSKIY, L.N. (1971): Eucryptite in petalite–microcline pegmatite of Soviet central Asia. *Dokl. Acad. Sci. USSR, Earth Sci. Sect.* **197**, 143-146.
- \_\_\_\_\_ & MATROSOV, I.I. (1974): Pseudomorphs of quartz and spodumene after petalite and their importance to the pegmatite-forming process. *Dokl. Acad. Sci. USSR, Earth Science Sect.* **216**, 164-166.
- SEBASTIAN, A. & LAGACHE, M. (1991): Experimental study of lithium-rich granitic pegmatites. I. Petalite + albite + quartz equilibrium. *Am. Mineral.* **76**, 205-210.
- SHEARER, C.K., PAPIKE, J.J. & JOLLIFF, B.L. (1992): Petrogenetic links among granites and pegmatites in the Harney Peak rare-element granite – pegmatite system, Black Hills, South Dakota. *Can. Mineral.* **30**, 785-809.
- STEWART, D.B. (1978): Petrogenesis of lithium-rich pegmatites. *Am. Mineral.* **63**, 970-980.
- WEBBER, K.L., SIMMONS, W.B., FALSTER, A.U. & FOORD, E.E. (1999): Cooling rates and crystallization dynamics of shallow level pegmatite–aplite dikes, San Diego County, California. *Am. Mineral.* **84**, 708-717.
- WHITWORTH, M.P. & RANKIN, A.H. (1989): Evolution of fluid phases associated with lithium pegmatites from SE Ireland. *Mineral. Mag.* **53**, 271-284.
- WOOD, S.A. & WILLIAMS-JONES, A.E. (1993): Theoretical studies of the alteration of spodumene, petalite, eucryptite and pollucite in granitic pegmatites: exchange reactions with alkali feldspars. *Contrib. Mineral. Petrol.* **114**, 255-263.
- WORDEN, R.H., WALKER, F.D.L., PARSONS, I. & BROWN, W.L. (1990): Development of microporosity, diffusion channels and deuteric coarsening in perthitic alkali feldspars. *Contrib. Mineral. Petrol.* **114**, 507-515.

*Received December 21, 1998, revised manuscript accepted May 7, 2001.*